

Available online at www.sciencedirect.com**ScienceDirect**

Energy Procedia 74 (2015) 130 – 138

Energy

Procedia

International Conference on Technologies and Materials for Renewable Energy, Environment and Sustainability, TMREES15

Performance of a Single Effect Solar Absorption Cooling System (LiBr-H₂O)

Omar Ketfi^{a,b*}, Mustapha Merzouk^a, Nachida Kasbadji Merzouk^b, Said El Metenan^b^a Laboratory for Fundamental and Applied Physics, University of Blida 1, W. Blida, Algeria^b Unité de Développement des Equipements Solaires/UES, Centre de Développement des Energies Renouvelables/CDER, 42415, W. Tipaza, Algérie

Abstract

Fossil fuels are on the verge of depletion, and the world energy consumption is in constant progression, resulting in very serious concerns about environmental issues. Mechanical refrigeration based on vapor compression principle uses high grade electrical energy, and refrigerant fluid with a global warming and ozone depletion potentials. Absorption machines using solar thermal energy are excellent alternatives to mechanical refrigeration. Absorption cooling systems are mature technologies that proved their abilities to provide clean cooling with the use of low grade solar and waste heat. In this paper we presented a modeling and simulation study of a 70 kW Yazaki absorption cooling machine working with water-lithium bromide mixture. The influence of different parameters (Heat exchanger efficiency, Generator, absorber and condenser temperatures) on the system performance is showed.

© 2015 The Authors. Published by Elsevier Ltd. This is an open access article under the CC BY-NC-ND license (<http://creativecommons.org/licenses/by-nc-nd/4.0/>).

Peer-review under responsibility of the Euro-Mediterranean Institute for Sustainable Development (EUMISD)

Keywords: Vapor Mechanical refrigeration; waste heat; clean cooling; absorption; water-lithium bromide mixture; Heat exchanger efficiency; system performance.

1. Introduction

Nowadays, the needs for thermal comfort in housing and office buildings generate a strong increase in energy demand especially during summertime. Air conditioning systems are basically mechanical vapor compression types, which use high grade electrical energy generated in power stations using fossil fuels.

* Corresponding author. Tel.: +21324410200.

E-mail address: omar_k09@hotmail.fr

Nomenclature

| | | |
|--------|----------------------------|-------|
| E_f | Heat exchanger effeteness' | |
| F_R | Flow ratio | |
| COP | Coefficient of performance | |
| M, m | Mass flow rate | kg/s |
| P | Pressure | kpa |
| Q | Heat capacity | kW |
| X | Solution of concentration | % |
| W_p | Pump work | kW |
| H | Enthalpy | kJ/kg |

Indices

| | |
|--------|---------------------------|
| a | absorber |
| c | Condenser, Cooling |
| e | Evaporator |
| g | Generator |
| p | Pump |
| r | Refrigerant |
| ss, ws | Strong and weak solutions |

This situation presents a very serious handicap in isolated areas with non-interconnected electrical grid. For this reason, renewable energies are excellent alternatives.

The Absorption cooling systems are one of the ways to produce air conditioning only by using solar thermal source as driving energy. In the water-Lithium bromide absorption systems, the solution is first heated in the desorbed (generator), and the obtained superheated water vapor (refrigerant) flows to the condenser where heat is transferred to the environment.

The liquid is moved through the expansion valve and enters to the evaporator; the liquid refrigerant evaporates by absorbing the heat from the refrigerated space. The weak liquid in the absorber absorbs the vapor leaving the evaporator and heat is transferred from the mixture. The enriched refrigerant- solution is pumped to the pressure level in the generator, where the weak solution returns to the absorber by transferring heat to the strong solution by way of the intercooler (heat exchanger).

Many works were done to evaluate the performances of a solar cooling system working in water- lithium bromide pair, [1, 2]. In 2012 [2] Rosiek and al, evaluated the performance of a solar-assisted 70 kW single effect LiBr-Water chiller located in Spain and achieved a maximum COP of 0.6 and Ali and al, [2] assessed the performance of a 35 kW solar absorption cooling plant and reported maximum collectors' field efficiency of 49.2% and a COP of 0.81. Hammad and Zurigat, [3] described the performance of a 1.5 Ton solar cooling unit. The unit comprises a 14 m² flat-plate solar collector system and five shell and tube heat exchangers. The unit was tested in April and May in Jordan. The maximum value obtained for actual coefficient of performance was 0.85.

In 2013, G. Cascales and al. [4], studied the global modeling of an absorption system working with LiBr/H₂O assisted by solar energy. It satisfies the air-conditioning necessities of a classroom in an educational center in Puerto Lumbreras, Murcia, Spain. The absorption system uses a set of solar collectors to satisfy the thermal necessities of the vapor generator. A dynamic simulation model, for a solar powered absorption cooling system was developed, and validated using measured data. Yeung and al., [5] designed and installed a solar driven absorption chiller at the University of Hong Kong, this system included 4.7 kW absorption chiller, flat plate solar collectors with a total area of 38.2 m², water storage tank and the rest of the equipment. They reported that the collector efficiency was estimated at 37.5%, the annual system efficiency at 7.8% and an average solar fraction of 55%, respectively.

The objective of this work is to evaluate the performances of a Yazaki medium capacity solar cooling system using LiBr-water absorption chiller.

For the simulation of this plant, Matlab simulation software was used and the influence of system parameters on the coefficient of performance was studied.

2. Mathematical model

2.1. Absorption Chiller

To simplify the problem, we neglect the pump work, the pressure drop in components and lines, and assign saturation conditions to states numbers 1, 3, 6 and 8 (figure 1).

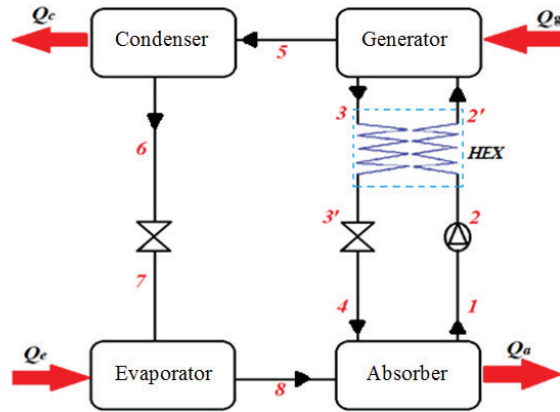


Figure 1. Simple effect Absorption cooling cycle

The properties are determined as follows. The mass flow of the refrigerant is equal to:

$$m_r = \frac{Q_e}{(H_8 - H_7)} \tag{1}$$

The ratio of the mass flow rate of the solution through the pump to the mass flow rate of the working fluid is defined as:

$$F_R = \frac{X_{ss}}{X_{ss} - X_{ws}} \tag{2}$$

It determines the needed energy to the pump. X_{ss} , X_{ws} are the strong and weak concentrations solutions respectively which can be determined from Merkel diagram [6].

The flow rate of the strong and weak solutions can be determined by:

$$m_{ws} = m_r F_R \tag{3} \quad \text{and} \quad m_{ss} = m_r (F_R - 1) \tag{4}$$

By using the first law of thermodynamic to each component of the absorption cycle including the condenser, evaporator, generator, absorber and the heat exchanger HEX, we can write:

For the Condenser:

$$Q_c = m_r (H_5 - H_6) \tag{5}$$

The vapor leaving the generator and entering the condenser is a superheated vapor. The enthalpy is expressed by [6]:

$$h_5 = 1.925T_g - 0.125T_c + 2365 \tag{6}$$

For the evaporator, equation (1) applies. In fact, the vapor leaving the evaporator is supposed saturated; so that, [6,8]:

$$H_8 = -0.00125397 * T_e^2 + 1.88060937 * T_e + 2500.559 \tag{7}$$

The energy balance in the Generator gives:

$$Q_g = m_c H_3 + m_r H_5 - m_d H_2 \quad (8)$$

For the Absorber we have:

$$Q_a = m_c H_4 + m_r H_8 - m_d H_1 \quad (9)$$

The enthalpies of the strong solution leaving the generator and the absorber are determined from Merkel Diagram, [6]. The energy balance in the Heat Exchanger gives:

$$Q_{ex} = m_{ss} (H_3 - H_3') = m_{ws} (H_2' - H_2) \quad (10)$$

Then the heat exchanger effectiveness is equal to:

$$E_f = \frac{T_3 - T_3'}{T_3 - T_2} \quad (11)$$

The Coefficient of performance (*COP*) of the whole system can be calculated by, [6,7]:

$$COP = \frac{Q_c}{Q_g + W_p} \quad (12)$$

If we neglect the pump work, we deduce:

$$COP = \frac{(H_8 - H_7)}{H_5 + (F_R - 1)H_3 - F_R H_2} \quad (13)$$

2.2 Solar collectors

In general, the required temperature for the absorption systems working with the solution pair Water-Lithium bromide is 70°C to 95 °C. For this reason, two types of solar collectors were considered: a high performance flat-plate solar collector and an evacuated solar tube collector. The formula used for flat-plate and evacuated-tube solar collectors' efficiency is [9,10]:

$$\eta_c = a_0 - a_1 \frac{(T_{moy} - T_{amb})}{I} - a_2 \left[\frac{(T_{moy} - T_{amb})}{I} \right]^2 \quad (14)$$

The useful energy collected by the solar collectors array is calculated by the following equation, [11]:

$$Q_{use} = IA\eta_c \quad (15)$$

Where Q_{use} , the useful energy gained by the solar collector array, I the solar radiation intensity in W, A the area of the collector in m², and η_c is the thermal efficiency of the solar collector array.

3. Results and discussion

The determination of the thermodynamic proprieties of each state in the cycle, the amount of heat transfer in each component, and the flow rates at different lines depends on the input parameters.

Taking example of Yazaki, [12] absorption machine WCF-SC20, the performances were simulated using the modelling tool Matlab 7.8 and the following input manufacturer data:

- Generator temperature, $T_g = 90$ °C

- Absorber temperature, $T_{amb} = 40$ °C

- Condenser temperature, $T_c = 40\text{ }^\circ\text{C}$
- Heat exchanger efficiency, $\eta_f = 0.7$
- Evaporator temperature, $T_e = 7\text{ }^\circ\text{C}$
- Refrigeration load, $Q_e = 70\text{ kW}$.

Table 1 shows the coefficients provided by the flat-plate collectors and the evacuated-tube collectors' manufacturer as determined from standard collector tests [13,14].

Table 1. Technical information of Cube-france solar collectors.

| | A_c | a_0 | a_1 | a_2 |
|---------------------------|--------------------|-------|-------|--------|
| Flat-plate collectors | 2.2 m ² | 0.776 | 3.66 | 0.0119 |
| Evacuated-tube collectors | 2.2 m ² | 0.776 | 3.66 | 0.0119 |

In figure 2 we can see the Matlab simulation interface. In all cases, the simulation results were compared with those published by L. Lansing, [16].

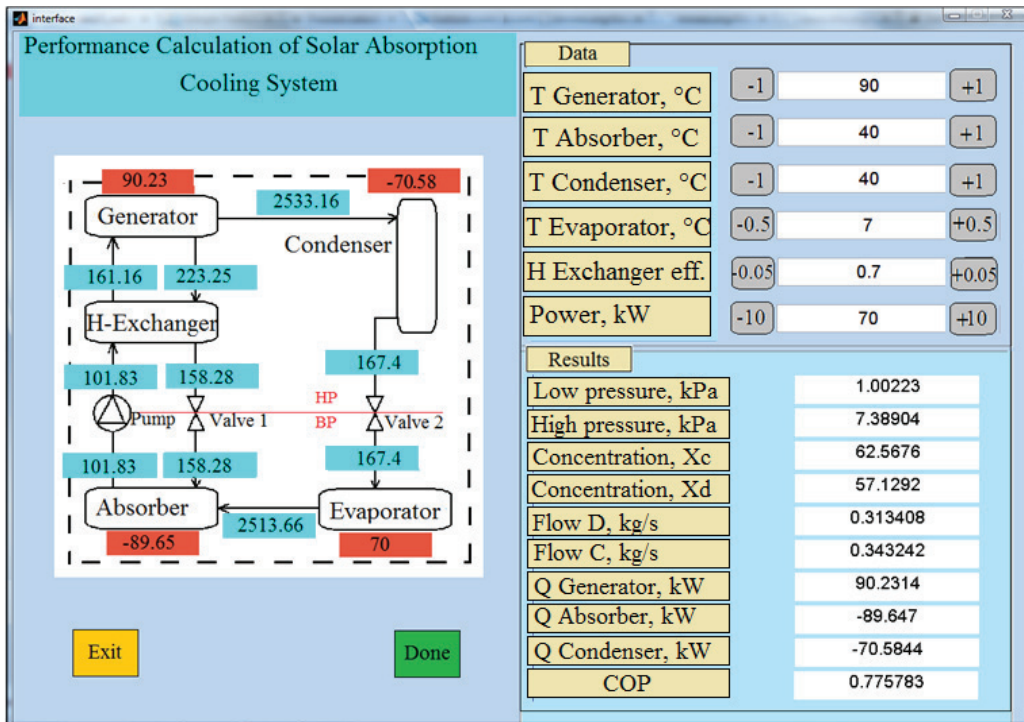


Figure 2. Interface of the Matlab simulation program.

3.1 COP function of T_g

The variation of the system's coefficient of performance and the flow ratio F_R with the generator temperature is shown in figure 3. As we can see, the COP of the system increase with the increase of the generator temperature, it means that the whole system performance goes better when T_g increase. However, due to the crystallization problem, the water- lithium bromide pair systems can't reach above $100\text{ }^\circ\text{C}$ [7]. The manufacturer gives an ideal coefficient of performance of the machine between 0.7 and 0.78, which is confirmed by the simulation for the previous initial conditions when the COP is found 0.75.

Compared with the simulation model done by L. Lansing, [16], the simulation results showed a good concordance.

F_R is an important design and optimizing parameter since it's directly related to the size and cost of the generator, absorber, heat exchangers and pump [10]. We can see that when the generator temperature increases, concentration of the strong solution increases, hence F_R decreases as can be seen in figure 3.

3.2 COP in function of T_c and T_a

Figure 4 shows that the COP of the system is decreasing with increasing the condenser and the absorber temperatures. Because the absorption of water by the Bromide Lithium is a chemical reaction that needs to be cooled for better efficiency, therefore decreasing the absorber temperature will improve the absorption reaction and the global system performances. For the condenser, the water vapor needs to be cooled for better condensation. The cooling can be done by using cooling towers or natural air cooling. For the water-lithium bromide pair, the use of the water for cooling purposes is more efficient than natural air cooling because of the major problem of crystallization. As shown in figure 4, the COP can reach his maximum value of 0.82 by decreasing the absorber and the condenser temperature down to 30°C.

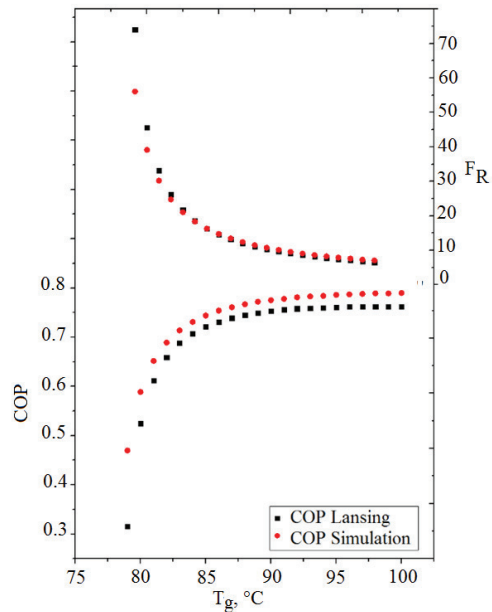


Figure 3. Variation of the COP and F_R with the generator temperature

3.3 COP in function of T_e

In Figure 5, the variation of COP with the evaporator temperature is shown. When the evaporator temperature rises, the amount of heat to extract is reduced. The result is an increase in the coefficient of performance of the system. This is one of the main reason why the Lithium bromide –water pair systems are well destined for air-conditioning activities that requires moderate temperatures.

3.4. COP function of E_f

Figure 6, shows that the system performance increases with the increase of the heat exchanger effectiveness. The heat exchanger helps to increase the strong solution temperature before entering to the generator, which will reduce the amount of energy required. With increasing the effectiveness of the heat exchanger, the energy needed in the generator decreases and this improve the COP of the system.

Figures 7 and 8 show the variation of the system coefficient of performance COP with the generator temperature for different value of heat exchanger efficiency (E_f). It is clearly shown that for higher heat exchanger effectiveness we obtain a higher COP. As we know, heat exchanger effectiveness depends on the type of heat exchanger. In absorption systems, double-pipe or shell-and-tube heat exchangers can be used. For these types of heat exchangers, the effectiveness can reach 0.8 to 0.85 max, [16].

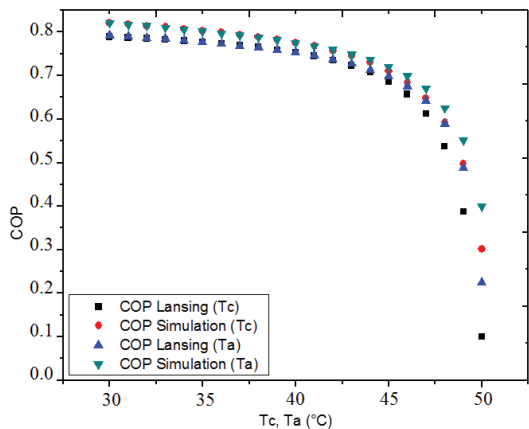


Figure 4 : Variation of the COP with the absorber and condenser temperatures

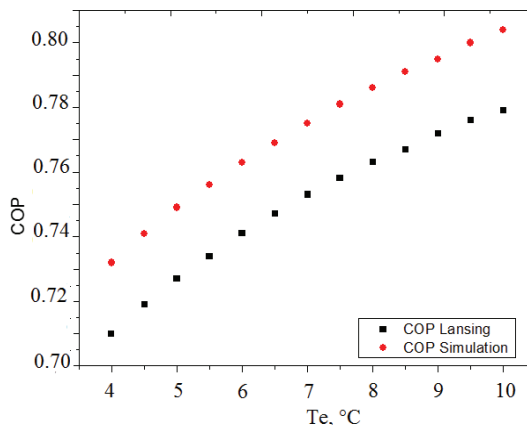


Figure 5 : Variation of the COP with the evaporator temperature

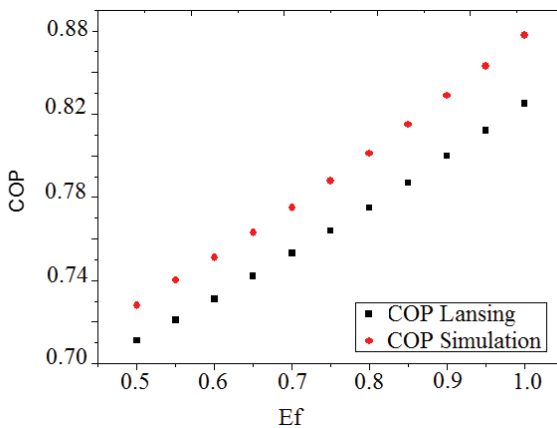


Figure 6 : Variation of the COP with the heat exchanger efficiency.

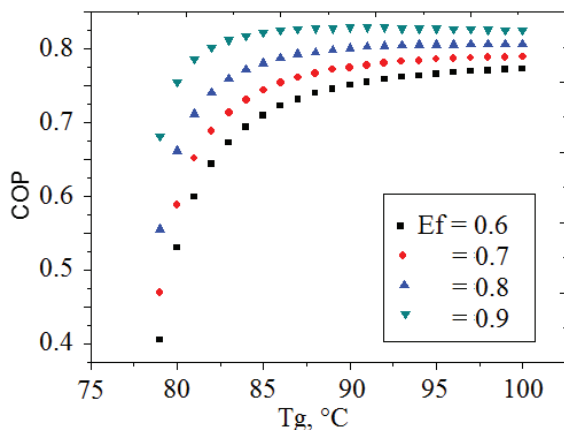


Figure 7: Variation of the COP with the generator temperature for different values of heat exchanger efficiency

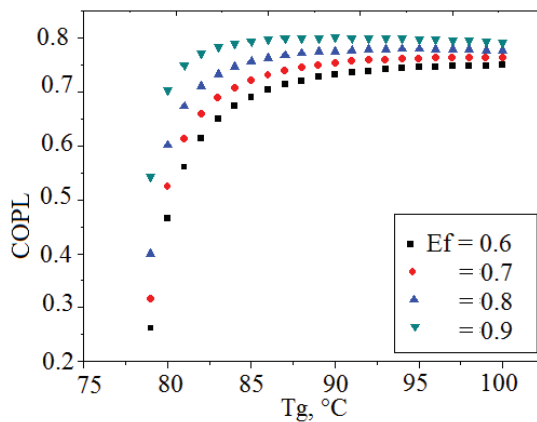


Figure 8 : Variation of the COP with the generator temperature for different values of heat exchanger efficiency for Lansing model.

4. Conclusion

In this study, a thermodynamic analysis of single stage absorption refrigeration system using water-lithium bromide pair was performed, and the theoretical results of the cycle were presented and compared with another mathematical model. Moreover, a simulation program using Matlab was developed in scope of this study. The simulation results showed that the COP of the cycle increases with increasing the generator and the evaporator temperatures, while, it decreases with the increase the condenser and the absorber temperatures. The COP of the system reached its maximum value of 0.77 with a generator temperature of $T_g = 92 \text{ }^\circ\text{C}$ that is close to the value given by the Yazaki manufacturer. Also the simulation study showed that for the manufacturer values, the absorption machine needs 90 kW for the generator supply witch is handled by 225.5 m² (2.5 m²/kW_{cool}) of Cube France flat plat solar collectors, and 175.1 m² (1.9 m²/kW_{cool}) of evacuated tubes solar collectors (Table1). That is close to the average value used for absorption systems 2.5 m²/kW_{cool} based on available information from current installations, [17]. The simulation results are compared and showed a very good concordance with those achieved by the mathematical model of L. Lansing, [16].

References

[1] Sury R. K., Al Madani K., Ayyash S., Choice of thermal energy system for solar absorption cooling, Solar Energy, Vol. 32, N°2, pp. 181-187, 1984.

[2] Darkwa J., Fraser S., Cow D.H.C., Theoretical and practical analysis of an integrated solar hot water-powered absorption cooling system, Energy, vol.39, Issue1, pp. 395-402, 2012.

[3] Florides G. A., Kalogiro S.A., Tassou S.AWrobel., L.C., Modeling and simulation of an absorption solar cooling system for Cyprus, Solar Energy, Vol. 72, N°1, pp. 43-51 2002.

[4] Gomri R., Simulation study of the performance of solar/natural gas absorption cooling chillers”, Energy Conversion and Management, Vol. 65, pp-675-681, 2013.

[5] Yeung M.R., Yueu P.K., Dunn A., Cornish L.S., Performance of a solar powered air conditioning system in Hong Kong, Solar energy, Vol. 48, N°5, pp. 309-319, 1992.

[6] ASHRAE fundamentals, Thermodynamic properties of refrigerant, Chapter 30, Inch-Pound Edition, 2009.

[7] Quiston M., Heating ventilating and air conditioning, Analyse and design, Sixth edition, Wiley, USA 2005.

[8] Hosseini L., Design and Analysis of a Solar Assisted Absorption Cooling System Integrated with Latent Heat Storage, Master thesis, Delft University of Technology, Holland, 2011.

[9] Duffie J. A., Beckman W. A., Solar engineering of thermal processes, Fourth Edition Sons and Wiley, New York, 2013.

[10]Karamangil M. I., Coskun S., Kaynakli O., Yamankaradeniz N., A simulation study of performance evaluation of single-stage absorption refrigeration system using conventional working fluids and alternatives, Renewable and sustainable Energy Review, Vol. 14, pp. 1969-1978, 210 Elsevier 2010.

[11] Kasbadji Merzouk N., Contribution à la détermination des performances théoriques et expérimentales de trois capteurs solaires plans, Magister thesis, HCR, Algiers 1986.

[12] Yazaki, Absorption cooling machine WFC-SC20, YAZAKI Europe Limited 2007.

[13] CubeFrance, Heat pipe evacuated tube solar collectors, Technical sheet, www.CubeFrance.fr

[14] CubeFrance, High performance flat plate solar collectors, technical sheet; www.CubeFrance.fr

[15] Kays W. M., London A. L., Compact Heat Exchangers, Ed. Krieger Pub. Co. 1984.

[16] Lansing F. L., Computer modeling of a single-stage Lithium Bromide/Water absorption refrigeration unit, JPLDeep Space Network Progress Report, 42-32, pp. 247-257, 1978.

[17] Martinez P. J., Martinez J. C., Lucas M., Design and test results of a low-capacity solar cooling system in Alicante (Spain), Solar Energy, Vol. 86, PP. 2950-2960, 2012.

Appendix

- Oldham diagram [6]
-

$$T = \sum_0^3 B_n X^n + T' \sum_0^3 A_n X^n \quad \text{and} \quad T'' = \left(T - \sum_0^3 B_n X^n \right) / \sum_0^3 A_n X^n$$

$$\log(P) = C + \frac{D}{T''} + \frac{E}{T''^2} \quad \text{With } T'' \text{ en K} \quad \text{and} \quad T'' = \frac{-2C_3}{C_2 + [C_2^2 - 4C_3(C_3 - \log(P))]}^{0.5}$$

| | | | | | |
|-------|--------------|-------|--------------|-------|-----------|
| A_0 | -2.00755 | B_0 | 124.937 | C_1 | 7.05 |
| A_1 | 0.16976 | B_1 | -7.71649 | C_2 | -1596.49 |
| A_2 | -0.003133362 | B_2 | 0.152286 | C_3 | -104095.5 |
| A_3 | 1.97668 E-5 | B_3 | -7.95090 E-4 | | |

Only use when $-15 < T' < 110$ °C , $5 < T < 175$ °C and $45 < X < 70\%$ of LiBr

- *Merkel diagram*, [6]

$$H = \sum_0^4 A_n X^n + T \sum_0^4 B_n X^n + T^2 \sum_0^4 C_n X^n$$

| | | | | | |
|-------|--------------|-------|--------------|-------|----------------|
| A_0 | -2024.33 | B_0 | 18.2829 | C_0 | -0.037008214 |
| A_1 | 163.309 | B_1 | -1.1691757 | C_1 | 0.0028877666 |
| A_2 | -4.88161 | B_2 | 0.03248041 | C_2 | -8.1313015 E-5 |
| A_3 | 0.06302948 | B_3 | -4.034184E-4 | C_3 | 9.9116628E-7 |
| A_4 | -2.913705E-4 | B_4 | 1.8520569E-6 | C_4 | -4.4441207E-9 |

Only use when $15 < T < 165$ °C and $45 < X < 70\%$ of LiBr